

DOI: 10.1002/adma.200502341

Solution and Surface Composition Gradients via Microfluidic Confinement: Fabrication of a Statistical-Copolymer-Brush Composition Gradient**

By Chang Xu, Susan E. Barnes, Tao Wu, Daniel A. Fischer, Dean M. DeLongchamp, James D. Batteas, and Kathryn L. Beers*

Materials and surfaces with composition gradients are of great importance for applications such as manipulating the motion of liquids or cells,^[1,2] directing the growth of neurons,^[3] and guiding the path of radiation.^[4] Within the last decade, the application of combinatorial methods in materials science has further increased interest in composition gradients.^[5] For example, gradient surfaces of poly(ethylene glycol) (PEG) and proteins have been used to study the interaction between cells and surfaces.^[6–8] The study of phase behavior in polymer blends and metal alloys has also been greatly accelerated by gradient specimens.^[9,10]

Several methods have been developed to make chemical-composition gradients, including the diffusion of molecules in gases or gels.^[1,11] Gradients have also been prepared by ion/metal deposition or ultraviolet–ozone irradiation.^[10,12] The use of scanning probe microscopy to form gradients at the nanometer scale has been explored.^[13] Recently, microfluidic networks were applied to generate complex discrete gradients in solution.^[14,15] Through surface-active components, gradients established in solutions were readily transferred onto surfaces.^[14,16]

Here, we introduce a facile method to generate solutions with continuous composition gradients using microfluidic techniques. The uniqueness of this approach is the ability of a

microchannel to preserve solution gradient profiles over a long period of time. The solution gradient inside the microchannel is generated by continuously changing the relative flow rates of the input solutions as the channel is filled. Once the flow inside the microchannel ceases, the only mixing is diffusive. Since liquid diffusion is relatively slow at room temperature, it is possible for certain reactions to complete before any significant change in the gradient profile takes place. Therefore, the microchannel provides a reaction environment in which different locations within the channel have different solution compositions.

To demonstrate the power of this technique, a gradient in a statistical-copolymer-brush composition was synthesized from a solution gradient of two monomers (*n*-butyl methacrylate (BMA) and 2-(*N,N*-dimethylamino)ethyl methacrylate (DMAEMA)). Our fabrication of a statistical-copolymer-brush gradient is an important advance beyond existing techniques because it enables the intimate mixing of different monomers, leading to broad sequence distributions in the polymer chains and the trapped expression of complex chemistries at the air interface. Polymer brushes also provide a thicker layer of protection for the hydrolytically unstable silicon–oxygen–carbon bonds at the substrate interface as compared to self-assembled monolayers (SAMs) alone. Surface-grafted polymers provide a robust means to control the surface properties such as wetting, cell adhesion, and alignment of block-copolymer microdomains.^[17–19] In this work, surface-initiated atom transfer radical polymerization (ATRP)^[20] was used to transfer the characteristics of the solution gradient onto the surface.

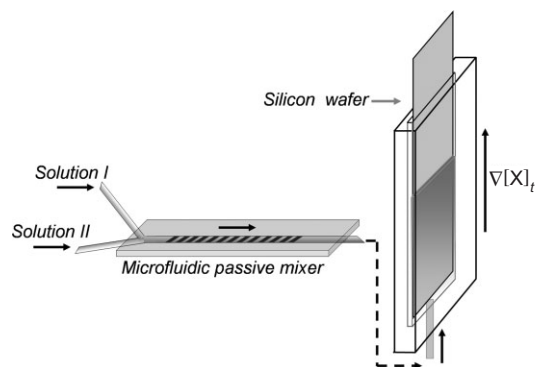
The setup employed to generate solution gradients is illustrated in Scheme 1. Two syringes containing different solutions (Ia or Ib and II) were mounted on separate syringe pumps, which were individually programmed to control the infusion rate and relative volumes of the solutions. Each syringe was connected to one of two inlets of a microfluidic passive mixer.^[21] The outlet of the mixer was connected to the bottom of a channel that was held upright. The channel had inner dimensions of 0.5 mm × 15 mm × 68 mm and was formed by placing a silicon wafer into a slender cuboid glass vessel. The solution gradient inside the channel was established by manipulating the relative infusion rates of the two solutions. In our experiments, the infusion started with pumping only solution I at a rate of 0.3 mL min⁻¹. The pumping rate

[*] Dr. K. L. Beers, Dr. C. Xu, Dr. S. E. Barnes, Dr. T. Wu, Dr. D. M. DeLongchamp
Polymers Division, National Institute of Standards and Technology
Gaithersburg, MD 20899 (USA)
E-mail: beers@nist.gov

Dr. D. A. Fischer
Ceramics Division, National Institute of Standards and Technology
Gaithersburg, MD 20899 (USA)

Prof. J. D. Batteas
Department of Chemistry, Texas A&M University
College Station, TX 77842 (USA)

[**] Contribution of the National Institute of Standards and Technology. Not subject to copyright in the United States. This work was carried out in the NIST Combinatorial Methods Center (NCMC). More information can be found at www.nist.gov/combi. D.M.D. acknowledges the NIST/NRC fellowship program for funding and thanks Sharadha Sambasivan of NIST for her help. Equipment and instruments or materials are identified in the paper to adequately specify the experimental details. Such identification does not imply recommendation by NIST, nor does it imply the materials are necessarily the best available for the purpose.



Scheme 1. Experimental setup for the formation of solution gradients inside a microchannel. Black arrows indicate the flow direction. $\nabla[X]_z$: change in concentration of solution X, with position, z .

of solution I was gradually decreased to 0 mL min^{-1} while the pumping rate of solution II was simultaneously increased to 0.3 mL min^{-1} , maintaining a constant overall flow rate of 0.3 mL min^{-1} . As the mixed solution entered the microchannel, the fluid was kept level by gravity. The flow stopped once the channel was filled. As a result, the solution in the upper portion of the channel was rich in solution I and in the lower portion of the channel was rich in solution II.

Raman spectroscopy verified the establishment and stability of the solution gradient inside the microchannel (Fig. 1). The two solutions used to generate the composition gradient both contained the same amount of water (5% by volume) and isopropyl alcohol (45% by volume). Isobutyric acid *n*-butyl ester (IABE, 50% by volume, solution Ib) and DMAEMA (solution II) were used as the ‘monomers’ in the two solutions. BMA (solution Ia) was replaced with IABE (a hydrogenated analogue) to reduce overlap in the vinyl and carbonyl stretching region (1800 to 1600 cm^{-1}) and improve resolution of the concentration variations across the channel. Raman spectra from selected locations along the gradient were acquired and normalized to the relative intensities of the solvent band at 814 cm^{-1} . The data (2000 to 1000 cm^{-1}) were then input into a three-factor partial least squares (PLS) calibration model for subsequent determination of solution composition.^[22,23]

Figure 1a shows the change in the Raman spectra along the gradient. An increase in the vinyl stretching mode at 1636 cm^{-1} was correlated with an increasing DMAEMA concentration in the gradient. Changes in intensity of the carbonyl stretching band at 1715 cm^{-1} were also observed with the changing solution composition. Figure 1b shows the DMAEMA solution composition determined from the spectral data as a function of its position inside the microchannel. From the bottom to the top of the microchannel, the DMAEMA monomer fraction was observed to decrease from 96 to 2% by volume.

The solution gradient should be relatively stable inside the microchannel. The stability of the gradient was confirmed by Raman spectroscopy of the solution composition inside the channel two hours after the generation of the gradient. Within

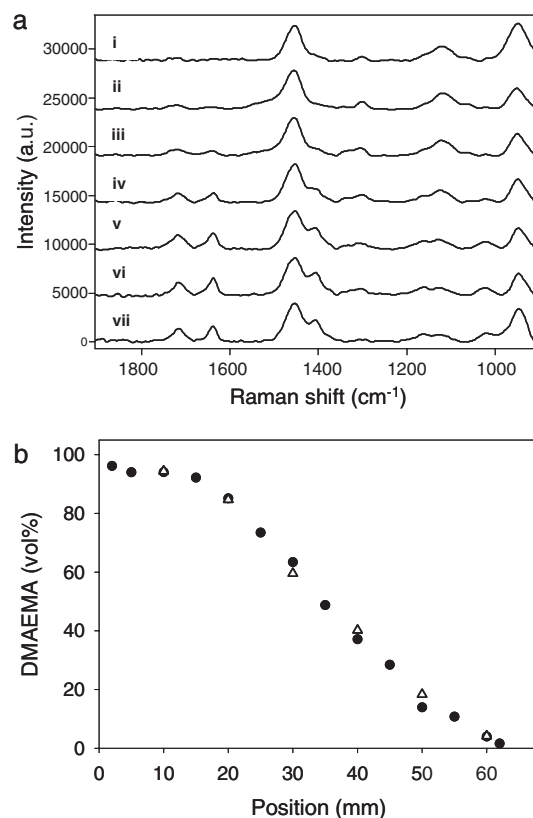


Figure 1. Determination of the solution gradient by Raman spectroscopy. a) Representative Raman spectra: i) 100% by volume of the monomer fraction isobutyric acid *n*-butyl ester (IABE) solution, ii) 6, iii) 5, iv) 3.5, v) 2, and vi) 0.5 cm from the bottom of the gradient, vii) 100% by volume DMAEMA solution. b) Measured vol% of the monomer fraction DMAEMA from Raman spectra as a function of position in the channel immediately after generation (●) and two hours later (△).

experimental uncertainty ($\pm 2.1\%$ by volume), there was no detectable change in solution composition along the length of the channel. Thus, the established gradient was stable under the experimental conditions (40 min at room temperature) used to fabricate the statistical-copolymer-brush gradient.

Monomers polymerized by the same mechanism in the same solution result in polymer chains with sequence distributions related to both the feed ratio of the monomers in solution and their reactivity ratios. When a radical mechanism is used, most monomer pairs tend to have similar reactivity ratios, which leads to a statistical distribution of repeat units in the chain that closely reflects the monomer feed ratio.^[24] This broad distribution of repeat units leads to some unique behavior of statistical copolymers. There are two particular observations with respect to grafted polymer chains. First, because the initiator concentration is extremely low and all of the chains grow simultaneously by the ATRP method, the monomer feed ratio is never altered by the polymerization, leading to a constant and uniform instantaneous chain composition. Second, most statistical copolymers should not exhibit the same surface rearrangements and segregation that have been recently studied in block-^[25–27] or tapered-copolymer^[28]

brushes. This is particularly useful when mixtures of chemical moieties are desired at the surface and their chemical expression needs to be trapped over long times or under varied conditions.

Copolymerization of BMA and DMAEMA via room temperature ATRP, which has been studied in solution,^[29] was selected for this study. As these solutions have similar concentrations to the solutions used in the Raman measurements and BMA is similar in molecular mass and structure to IABE, these monomer-solution gradients should behave similarly to the model system described above. The silicon substrate inside the microchannel was functionalized with a SAM of 11-(2-bromo-2-methyl)propionyloxy-undecyltrichlorosilane, an ATRP initiator.^[30] The channel was quickly filled (<2 min) to minimize polymerization during the infusion. After 40 min of polymerization at room temperature, the silicon substrate was removed from the vial and the reaction was stopped by immediate rinsing with *N,N*-dimethylformamide and ethanol before the slide was dried under a flow of nitrogen.

Figure 2 shows the thickness profiles of the statistical-copolymer gradient as measured by ellipsometry. Polymerization from the surface resulted in polymer brushes with thick-

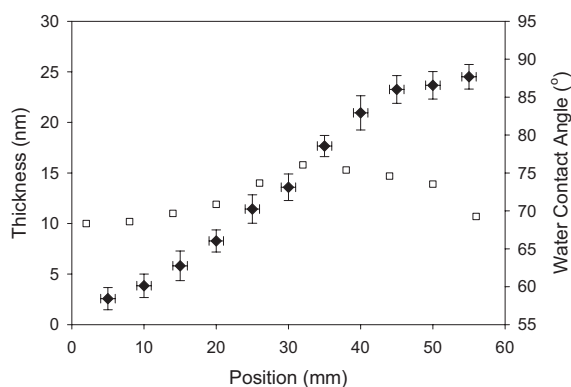


Figure 2. Thickness (□) and static water contact angle (◆) profiles of the statistical copolymer brushes PBMA-*co*-PDMAEMA along a composition gradient, which were synthesized from a solution with a monomer concentration gradient. The error bars for the water-contact-angle data represent two standard uncertainties based on nine repeated measurements. The error bars for the position measurements represent two standard uncertainties based on the visual accuracy of droplet positioning and the droplet size.

nesses ranging from 10 to 16 nm at different locations. Slightly elevated thicknesses were reproducibly observed for intermediate monomer feed ratios. We don't fully understand what caused this, but it might be attributed to small variations in polymerization rates or possibly slight exposure to oxygen at the inlet and outlet of the reactor.

Surface water contact angle measurements were used to evaluate the gradient profile of the surface. Homopolymer brushes of PBMA and PDMAEMA have distinct surface wetting behaviors: the static water contact angles for homopolymer brushes of PDMAEMA and PBMA synthesized under

the same conditions were 60° and 89°, respectively. Mapping the gradient substrate using the static water contact angle measurement revealed the gradual change from the characteristic value of PDMAEMA to that of PBMA, suggesting a gradual variation in the surface chemical composition across the length of the substrate. The same gradient in contact angles was measured after several hours and after several months, indicating a very stable mixed interface.

Chemical variation across the surface was directly confirmed with near-edge X-ray absorption fine structure (NEXAFS) spectroscopy, which is sensitive to elemental composition and bond hybridization.^[31] NEXAFS spectroscopy is well suited to the characterization of combinatorial gradients^[32] and was used here to measure the nitrogen K-edge unique to PDMAEMA in the experiment. A spectrum was collected every 0.5 mm along the gradient surface, as shown in Figure 3, revealing a gradient in elemental nitrogen density. The nitrogen density within the sampled volume is proportional to the overall partial electron yield (PEY) intensity across the nitro-

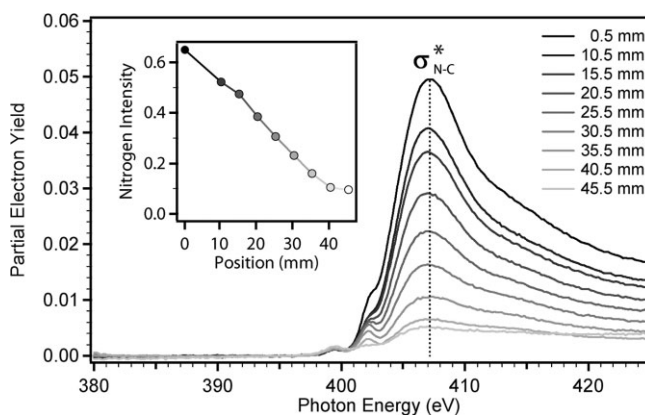


Figure 3. NEXAFS spectroscopy analysis for the statistical-copolymer brush, PBMA-*co*-PDMAEMA, composition gradient. The inset shows the linear variation of nitrogen density with position.

gen K-edge, obtained by integrating a spectrum over all transitions. The primary transition is the carbon–nitrogen 1s \rightarrow σ^* , consistent with the DMAEMA nitrogen orbital hybridization. The nitrogen density varies linearly with position, as shown in the inset of Figure 3. The spectral shapes at all positions are similar, indicating that the nitrogen density originates only from PDMAEMA. NEXAFS chemical analysis confirmed that the monomer solution gradient established by microfluidic mixing created a precisely controlled gradient of statistical copolymers.

In summary, a general method to establish solution composition gradients by means of microfluidics was developed. The generation and maintenance of a gradient inside a microchannel was verified by Raman spectroscopy. Utilizing surface-initiated polymerization, the monomer solution gradient of BMA and DMAEMA was successfully applied to synthesize a statistical-copolymer-brush composition gradient. The formed gra-

dient was confirmed by water-contact-angle measurements and NEXAFS spectroscopy. Our results indicate that microchannels can be used as a unique reaction environment for the fabrication of surface materials with well-defined composition gradients. Gradients in statistical-copolymer composition have excellent potential to accelerate discovery and understanding of a number of interfacial phenomena relevant to nanotechnology, microfluidics, electronics, and biology.

Experimental

The design of the chaotic passive microfluidic mixer, which contained obliquely oriented ridges on one wall of the channel, was based on the geometry reported by Whitesides and co-workers [21]. The channel was sandwiched between two glass slides. The other two sides of the channel and the ridges were fabricated by frontal photopolymerization of a commercial thiolene-based optical adhesive (NOA 81, Norland Products) according to procedures described previously [33,34].

The formation of SAMs with ATRP-initiating moieties was described in previous reports [35]. The polymerization solutions were prepared according to the following procedures. CuBr (21 mg), bipyridine (49 mg), and a magnetic stirring bar were added to a flask capped with a rubber septum. After three cycles of pulling vacuum followed by backfilling with argon, degassed isopropyl alcohol (4.5 mL), degassed H₂O (0.5 mL), and degassed monomer (5.0 mL; BMA for solution I and DMAEMA for solution II) were sequentially syringed into the flask. The polymerization mixtures were stirred for 1 h before they were transferred into the syringes.

Raman data were obtained using a Raman systems R2001 spectrometer (Ocean Optics, Inc.) with a 785 nm laser excitation and a charge-coupled device (CCD) detector. Individual spectra from the gradient were obtained by focusing a noncontact fiber-optic probe (nominal focal length of 5 mm and 200 mm focal size) into the channel at various points on the substrate. Data were acquired over two-minute intervals at a resolution of 10 cm⁻¹ and were analyzed using commercial software (Grams AI). Chemometric modeling of the spectra was conducted by PLS using Grams-PLS IQ.

For determination of component concentration in the gradient, a PLS calibration was constructed from spectra of standard solutions acquired in the device. Spectral data (1800 to 1000 cm⁻¹) of standards containing DMAEMA (0 to 100% by volume, in 25% increments) were used alongside the associated concentration values to produce a three-factor PLS calibration model ($R^2=0.998$). The model was constructed using raw data as acquired from the device normalized to the solvent band at 815 cm⁻¹ with no further pretreatment. The standard error was calculated to be $\pm 2.1\%$ by volume DMAEMA (1σ). Determination of DMAEMA composition and gradient stability in the channel was subsequently conducted by reference to the chemometric model.

Polymer-brush thickness was measured using a VASE ellipsometer (J. A. Woollam Co. Inc.; one standard uncertainty was measured as 0.2 nm). Surface water-contact-angle (θ_w) measurements were carried out with a Krüss G2 contact-angle goniometer. NEXAFS spectra were collected at the NIST/Dow soft X-ray characterization facility at the National Synchrotron Light Source, Brookhaven National Laboratory. Experimental conditions included orientation-insensitive beam incidence at 54.7° and a PEY grid bias of -280 V.

Received: November 1, 2005
Final version: February 10, 2006
Published online: April 19, 2006

- [1] M. K. Chaudhury, G. M. Whitesides, *Science* **1992**, 256, 1539.
[2] J. T. Smith, J. K. Tomfohr, M. C. Wells, T. P. Beebe, T. B. Kepler, W. M. Reichert, *Langmuir* **2004**, 20, 8279.

- [3] S. K. W. Dertinger, X. Y. Jiang, Z. Y. Li, V. N. Murthy, G. M. Whitesides, *Proc. Natl. Acad. Sci. USA* **2002**, 99, 12542.
[4] A. Papp, H. Harms, *Appl. Opt.* **1975**, 14, 2406.
[5] X.-D. Xiang, I. Takeuchi, *Combinatorial Materials Synthesis*, Marcel Dekker, New York **2003**.
[6] K. Mougou, A. S. Ham, M. B. Lawrence, E. J. Fernandez, A. C. Hillier, *Langmuir* **2005**, 21, 4809.
[7] S. T. Plummer, Q. Wang, P. W. Bohn, R. Stockton, M. A. Schwartz, *Langmuir* **2003**, 19, 7528.
[8] S. Kramer, H. Xie, J. Gaff, J. R. Williamson, A. G. Tkachenko, N. Nouri, D. A. Feldheim, D. L. Feldheim, *J. Am. Chem. Soc.* **2004**, 126, 5388.
[9] J. C. Meredith, A. Karim, E. J. Amis, *Macromolecules* **2000**, 33, 5760.
[10] Y. K. Yoo, F. W. Duwey, H. Yang, D. Yi, J.-W. Li, X.-D. Xiang, *Nature* **2000**, 406, 704.
[11] B. Liedberg, M. Wirde, Y. T. Tao, P. Tengvall, U. Gelius, *Langmuir* **1997**, 13, 5329.
[12] S. V. Roberson, A. J. Fahey, A. Sehgal, A. Karim, *Appl. Surf. Sci.* **2002**, 200, 150.
[13] R. R. Fuierer, R. L. Carroll, D. L. Feldheim, C. B. Gorman, *Adv. Mater.* **2002**, 14, 338.
[14] N. L. Jeon, S. K. W. Dertinger, D. T. Chiu, I. S. Choi, A. D. Stroock, G. M. Whitesides, *Langmuir* **2000**, 16, 8311.
[15] S. K. W. Dertinger, D. T. Chiu, N. L. Jeon, G. M. Whitesides, *Anal. Chem.* **2001**, 73, 1240.
[16] X. Jiang, Q. Xu, S. K. W. Dertinger, A. D. Stroock, T.-m. Fu, G. M. Whitesides, *Anal. Chem.* **2005**, 77, 2338.
[17] B. Zhao, W. J. Brittain, W. Zhou, S. Z. D. Cheng, *J. Am. Chem. Soc.* **2000**, 122, 2407.
[18] H. Ma, J. Hyun, P. Stiller, A. Chilkoti, *Adv. Mater.* **2004**, 16, 338.
[19] P. Mansky, Y. Liu, E. Huang, T. P. Russell, C. J. Hawker, *Science* **1997**, 275, 458.
[20] K. Matyjaszewski, J. Xia, *Chem. Rev.* **2001**, 101, 2921.
[21] A. Stroock, S. K. W. Dertinger, A. Ajdari, I. Mezic, H. A. Stone, G. M. Whitesides, *Science* **2002**, 295, 647.
[22] J. M. Chalmers, *Spectroscopy in Process Analysis*, Sheffield Academic, Sheffield, UK **2000**.
[23] I. R. Lewis, H. G. M. Edwards, *Handbook of Raman Spectroscopy: From the Research Laboratory to the Process Line*, Marcel Dekker, New York **2001**.
[24] A. E. Hamielec, J. F. Macgregor, E. Penlidis, *Comprehensive Polymer Science*, Vol. 3 (Eds: G. C. Eastmond, A. Ledwith, S. Russo, P. Sigwalt), Pergamon, London **1989**, Ch. 2.
[25] S. G. Boyes, A. M. Granville, M. Baum, B. Akgun, B. K. Mirous, W. J. Brittain, *Surf. Sci.* **2004**, 570, 1.
[26] I. Luzinov, S. Minko, V. V. Tsukruk, *Prog. Polym. Sci.* **2004**, 29, 635.
[27] C. Xu, T. Wu, J. D. Batteas, C. M. Drain, K. L. Beers, M. J. Fasolka, *Appl. Surf. Sci.* **2006**, 252, 2529.
[28] C. Xu, T. Wu, Y. Mei, C. M. Drain, J. D. Batteas, K. L. Beers, *Langmuir* **2005**, 21, 11136.
[29] S. B. Lee, A. J. Russell, K. Matyjaszewski, *Biomacromolecules* **2003**, 4, 1386.
[30] K. Matyjaszewski, P. J. Miller, N. Shukla, B. Immaraporn, A. Gelman, B. B. Luokala, T. M. Siclovan, G. Kickelbick, T. Vallant, H. Hoffmann, T. Pakula, *Macromolecules* **1999**, 32, 8716.
[31] J. Stöhr, *NEXAFS Spectroscopy*, Springer, Berlin **1992**.
[32] D. A. Fischer, K. Efimenko, R. R. Bhat, S. Sambasivan, J. Genzer, *J. Macromol. Rapid Commun.* **2004**, 25, 141.
[33] J. T. Cabral, S. D. Hudson, C. Harrison, J. F. Douglas, *Langmuir* **2004**, 20, 1020.
[34] Z. T. Cygan, J. T. Cabral, K. L. Beers, E. J. Amis, *Langmuir* **2005**, 21, 3629.
[35] C. Xu, T. Wu, C. M. Drain, J. D. Batteas, K. L. Beers, *Macromolecules* **2005**, 38, 6.